3 NACA0021 at 60$^{\text{o}}$ incidence

A. Garbaruk, M. Shur, M. Strelets, A. Travin (NTS)

3.1 Introduction

A flow over an airfoil in a deep stall is a typical example of the flows DES was designed for. Not surprisingly, exactly such a flow (NACA0012 airfoil at large angles of attack) was the first real 3D application of DES (Shur et al., 1999), and a success of this simulation to a considerable extend influenced the fast spreading of the DES technology. Note, however, that in this first DES application and also in the subsequent studies of this flow in the framework of FLOMANIA EU project, a comparison with experimental data was rather restricted, since only the integral lift and drag values were available. Other than that, because of the limited computer power, the computations were carried out with the use of relatively coarse grids and narrow domains in the spanwise direction. In the recent experimental study of the NACA0021 airfoil at 60$^{\text{o}}$ angle of attack (Swalwell et al., 2003, Swalwell, 2005) a much more informative database has been accumulated which includes not only mean flow characteristics but also lift and drag time histories and corresponding spectra. This database and, also, a significant increase of the computer power since 1999, open a possibility of a more reliable validation of different versions of DES and of new, non-conventional, URANS approaches (SAS of Menter and Egorov, 2005 and TRRANS of Travin et al., 2004) developed in the course of DESider. These considerations have motivated including of the NACA 0021 flow in the list of DESider test cases.

3.2 General flow description

The airfoil geometry normalized with the chord length, c, is defined by:

$$y = \pm \frac{0.21}{0.2} \left(0.2969\sqrt{x} - 0.126x - 0.3516x^2 + 0.2846x^3 - 0.1015x^4 \right)$$

Experimental flow parameters, needed to set up appropriate numerical simulations are presented in Table 1

Table 1 Flow parameters

Parameter	Notation	Value
Reynolds number	Re=$U_\infty c/\nu$	2.7x10^5
Chord length	c	0.125 m
Angle of attack	α	60^0
Free stream Mach number	M	0.1
Free stream streamwise turbulence intensity	l_u	0.6%

The experiments were carried out in the wind tunnel of Monash University (see Fig.1), which experimental section width is $7.2c$ and height is $16c$.
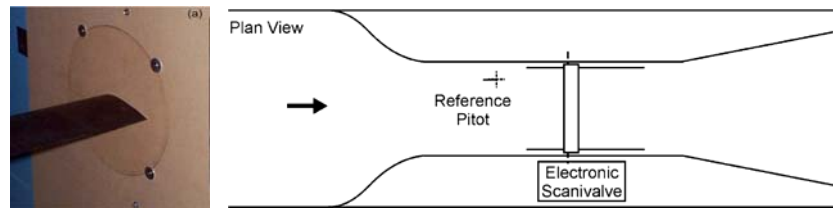

Figure 1 NACA0021 airfoil in wind tunnel (left) and a plan view of wind tunnel (right)

The flow parameters measured in the experiments and kindly provided to the DESider consortium by K. Swalwell are:

1. Time-averaged pressure coefficient distribution over the airfoil surface, $C_p(x)$;

2. Time- and span-averaged drag and lift coefficients, C_D, C_L;

3. Time histories of the sectional lift and drag coefficients (32,000 points total over the time interval $T \approx 9000(c/U_0)$).

3.3 Participants and some details of simulations

A list of participants and key information on turbulence modelling approaches and computational grids they used are presented in Table 2.

All the simulations, except for that of the EADS-M, were carried out without accounting the wind tunnel walls ("in free air"). Most of them used O-type grids ("coarse" and "fine") built by NTS and provided to all the interested partners. Along with this, NLR has built three (coarse, medium, and fine) structured grids, which were also used by DLR and TUB, and EADS-M generated an unstructured grid (examples of the grids are presented in Fig.2.) All the grids are uniform in the spanwise direction (information about the span-size of the domain, L_z, and the grid steps Δz in different simulations is presented in Table 2).
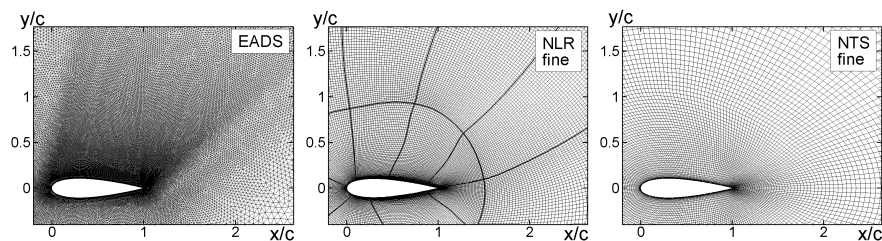

Figure 2 Zoomed fragments of different grids in *XY*-plane

All the simulations were conducted in the "fully-turbulent" mode, i.e., with prescription of relatively high eddy viscosity ($\nu_t \approx \nu$) at the inflow boundary, which ensures turbulent flow starting virtually from the leading edge of the airfoil. Other than that, in order to ensure a consistency of the comparison of the lift and drag spectra, all the partners computed these spectra with the use of the common Fourier transform tool provided by TUB.

Table 2 Summary of simulations

Partner	Model	Grid size (M nodes)	z-grid		Δt	Time Sample
			L_z	Δz		
ANSYS	SAS 2	1.9	4	0.03	0.03	400
DLR	S-A DDES	0.5	1	0.03	0.0125	320
		1.6	1	0.02	0.0125	345
		5.2	1	0.014	0.0125	280
EADS-M	S-A DES	19.2	7.2	0.025	0.07	429
IMFT	S-A DES	0.5	1	0.03	0.0024	48
	k-ω DES	0.5	1	0.03	0.0024	50
	k-ω OEM DES	0.5	1	0.03	0.0024	41
		2.0	4	0.03	0.0024	20
NLR	X-LES	0.5	1	0.03	0.0125	275
		1.6	1	0.02	0.0125	138
		5.2	1	0.014	0.0125	131
NTS	S-A DES	0.5	1	0.03	0.03	2500
		0.7	1.4	0.03	0.03	2000
		1.0	2.0	0.03	0.03	2000
		1.4	2.8	0.03	0.03	2000
		2.0	4	0.03	0.03	2000
		1.4	2	0.02	0.03	2000
		1.0	2	0.03	0.02	2000
		2.0	2	0.03	0.02	2000
	SAS 2	1.0	2	0.03	0.03	2000
	TRRANS	1.0	2	0.03	0.03	2000
NUMECA	S-A DES	0.5	1	0.03	0.0125	177
TUB	SALSA DES	0.5	1	0.03	0.025	1000
	CEASM DES	0.5	1	0.03	0.025	1620
		1.6	3.24	0.03	0.025	730
	LLR DES	0.5	1	0.03	0.025	1230
		0.5	1	0.03	0.0125	790
		1.6	1	0.02	0.0125	650
		5.2	1	0.014	0.0125	535

3.4   DES results and discussion

3.4.1   *Effect of time sample, span size of the domain, and wind-tunnel walls*

Starting from FLOMANIA it became clear that in order to obtain mean characteristics of the flows around nominally 2D bluff bodies, time-samples used for the averaging should be rather long. In order to get a quantitative information about the length of time-samples ensuring reliable averaging (this is of crucial importance for formulation of clear guidelines on DES of such flows), NTS and TUB conducted special numerical studies. Their major outcome is presented in Fig. 3 in a form of running average of the lift coefficient as a function of time at different span sizes of the domain from DES based on the S-A (NTS) and CEASM (TUB) background RANS models.
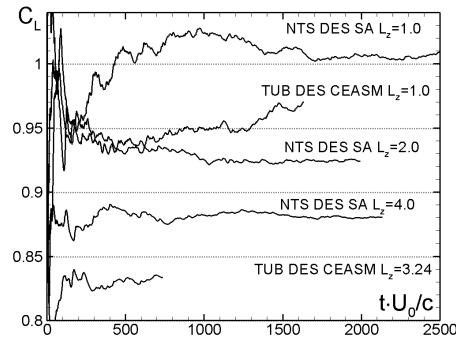

Figure 3 Running time-average of span-averaged lift coefficient predicted by DES on NTS coarse grid at different span size values

One can see that for both considered DES versions very long time-samples are needed to get a statistically reliable lift value. Note that because of the span-averaging, with the span size increase the demands to the time-sample for obvious reason become less severe but even for the largest of the considered span-sizes, 4c, the time-sample has to be not shorter than ~300-400 convective units. Therefore, some of the simulations (see Table 2) have insufficient time-samples. This circumstance should be kept in mind when comparing predictions of the mean forces with the experimental data.

   Another observation from Fig.3 is that the effect of the span size of the domain on the mean lift is rather strong and that saturation occurs at L_z about as large as 4c. This is more clearly seen in Fig. 4, where the mean pressure distributions and power spectral density (PSD) of the lift are presented from the simulations with different L_z. The figure suggests also that the span-independent mean pressure agrees with the data worse than that obtained with the narrower domains, 1c and 1.4c. This finding is frustrating. Indeed, provided that the experimental data are accurate, this, in fact, suggests that the earlier conclusions about a very high

accuracy of DES as applied to the massively separated 2D airfoil flows, which were based on the simulations carried out in relatively narrow domains, are somewhat too optimistic. However, as seen from the lift spectra in Fig.4, with the span-size increase, there is a clear trend to a better agreement of the spectra with the data, which obviously contradicts the worse agreement of the mean pressure.
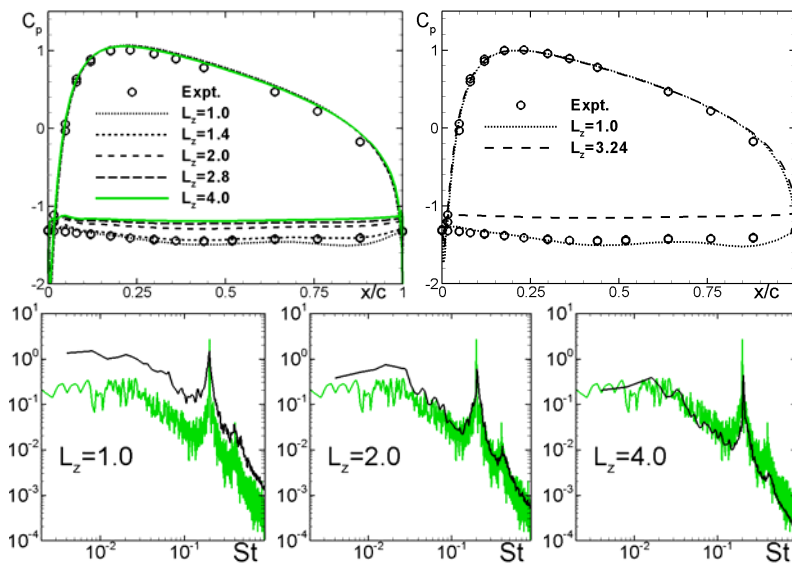

Figure 4 Upper row: mean pressure at different span-sizes of domain from S-A DES (left frame, NTS simulation) and from CEASM DES (right frame, TUB simulation). Lower row: PSD of lift coefficient (NTS, S-A DES); black lines – computation, green lines - measurements. Simulations on coarse NTS grid
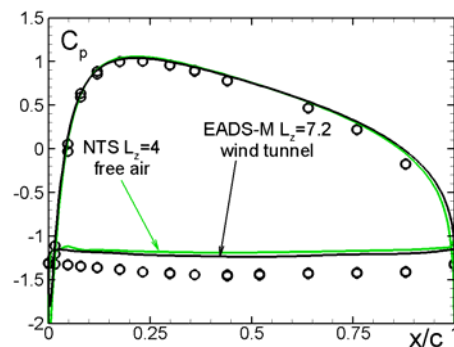

Figure 5 Comparison of Cp computed with periodic boundary conditions at L_z= 4c and for full span-size of the model with account of tunnel wall effects

Figure 5 compares the mean pressure predicted by NTS at $L_z = 4c$ with that of EADS-M obtained for the full span size of the experimental model (L_z=7.2c) with account of the walls of the experimental section. It shows that the effect of the walls is marginal: once the span-size of the domain is large enough, the simulation under the free-air conditions (with periodic boundary conditions in the spanwise direction) virtually coincide with those obtained with account of the walls. This is true not only with respect to the mean C_P distribution but also for the lift spectra shown in Fig. 6 (EADS-M spectrum is more "noisy" because it is a sectional spectrum, whereas the NTS one is span-averaged) and for the resolved turbulent kinetic energy shown in Fig. 7.
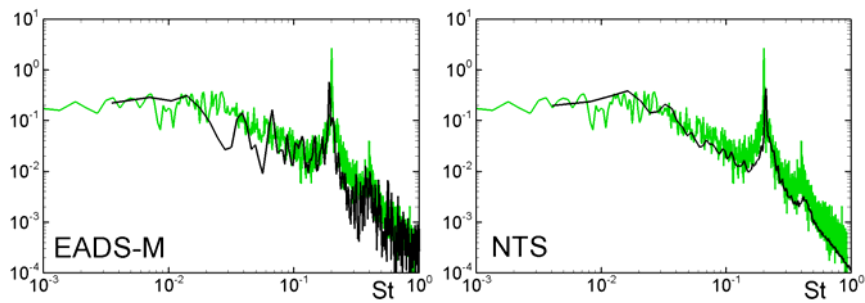
Figure 6 Comparison of computed (black lines) and experimental (green lines) PSD of lift coefficient. Left: EADS-M simulation with account of wind-tunnel walls, sectional spectrum; right: NTS simulation with periodic boundary conditions in the spanwise direction (L_z=4.0), span-averaged spectrum
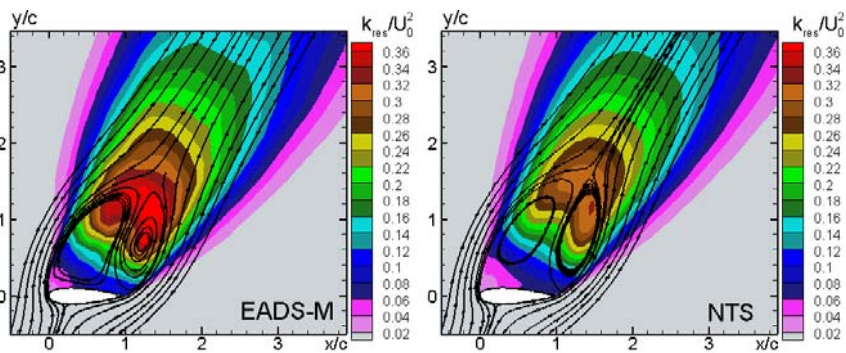
Figure 7 Mean-flow streamlines and resolved TKE fields (same simulations as in Fig.6)

3.4.2 Effect of background RANS model for DES

A relatively weak sensitivity of DES to a background RANS model demonstrated in the literature is an essential DES feature naturally considered as one of its serious advantages over RANS turbulence modelling. Results of the studies of the effect of the background RANS model on DES predictions of the NACA 0021 flow are summarized in Figs. 8-10. One can see that, indeed, the effect is marginal: the results obtained with the use of DES versions based on very different RANS models are close to each other in terms of both turbulence resolution and mean flow, thus supporting insensitivity of DES to the background RANS model at least in the situations, when prediction of the separation point, the RANS mode of DES is responsible for, is not challenging.
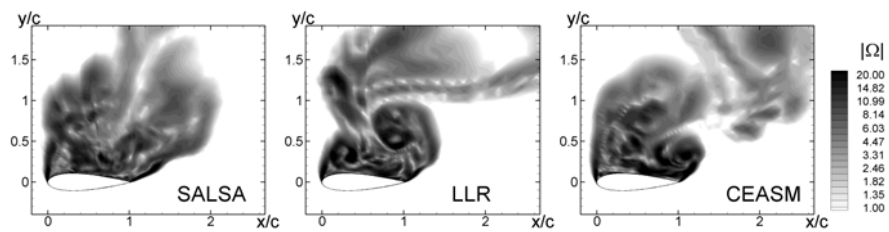

Figure 8 Snapshots of vorticity from DES based on different RANS models (simulations of TUB, coarse NTS grid, $L_Z=1$)
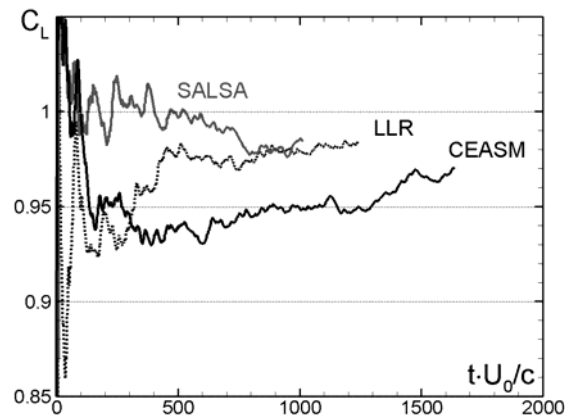

Figure 9 Running time-average of span-averaged lift coefficient from DES based on different RANS background models (same simulations as in Fig.8)
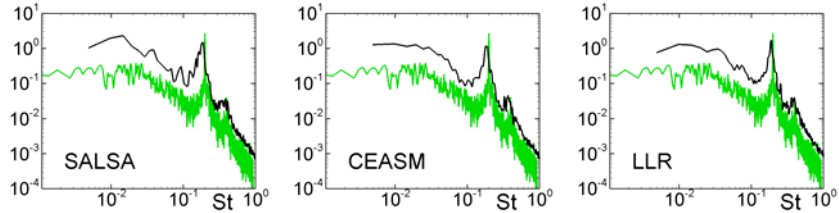
Figure 10 PSD of lift coefficient from DES based on different RANS background models (same simulations as in Fig.8). Black lines - simulations, green lines - data

3.4.3 Effect of grid-refinement

As far as the mean flow characteristics are concerned, the simulations carried out on very different grids (see Table 2) have given close results thus suggesting that even the coarse NTS grid provides for a sufficiently accurate mean flow prediction. This is illustrated by Fig.11, which compares the time- and span-averaged distributions of the pressure coefficients computed by NTS on its coarse (1 M nodes) and fine (2 M nodes) structured grids and by EADS-M on a very fine (19.2M nodes) unstructured grid.
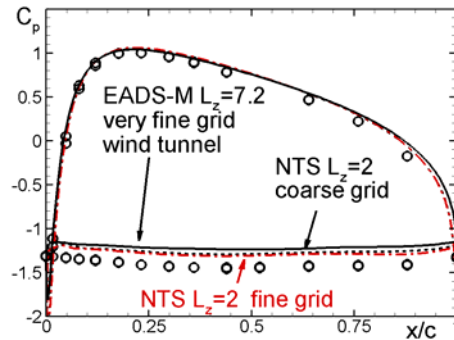

Figure 11 Effect of grid refinement on time- and span-averaged Cp distributions predicted by S-A DES

3.4.4 Cross-plotting of results

In this section we present a comparison of the available results. Considering the strong effect of the span-size of the domain L_z discussed above, in order to perform this comparison consistently, only results obtained in the simulations with the same L_z should be taken into account. A maximum number of such simulations is available at L_z=1.0. So the cross-plotting is carried out exactly for this L_z value.
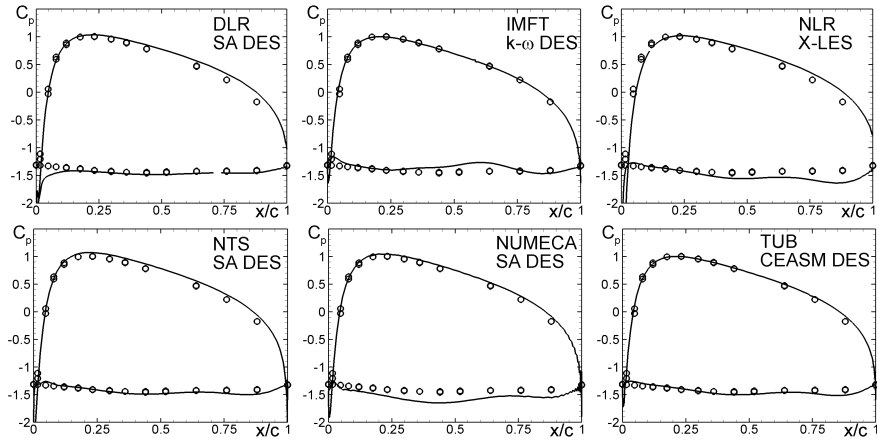
Figure 12 Pressure distributions computed by different partners. DLR, NLR: coarse NLR grid; other partners: coarse NTS grid
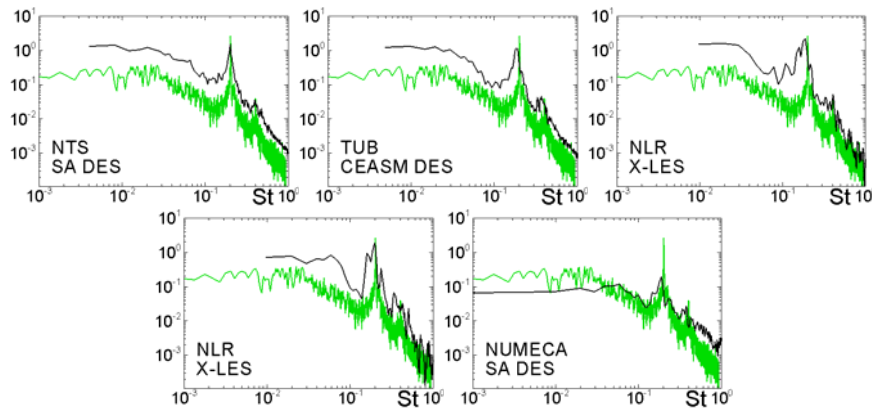

Figure 13 PSD of lift coefficient computed by different partners (same simulations as in Fig.12). Upper row: sectional spectra of C_L averaged over span; lower row: spectra of span-averaged C_L. Black lines - simulations, green lines – data

Figures 12-14 present respectively the mean pressure distributions, spectra of the lift coefficient, and streamlines and resolved turbulent kinetic energy computed by different partners with the use of different codes and different DES versions. Note that the experimental data for pressure and lift spectra are shown in the figures just as a reference: considering the strong effect of the span-size of the domain on the results of the simulations discussed above, at the span-size as low as L_z=1 comparison with the data is not quite representative. Also, when analysing these results, one should keep in mind that in the simulations of IMFT and NUMECA

the time samples used for the mean flow and spectra computation are too short (see Table 2). Other than that, similar to what has been done in the experiments, NTS and TUB computed the lift spectra by span averaging of the sectional spectra, whereas DLR, NLR, and NUMECA computed the spectra of the span-averaged lift, which is not quite the same. Nonetheless, even with all these differences, the results of different partners shown in Figs.12-14 are, in general, close to each other, which suggests a correct implementation of all the DES versions involved and a relatively weak sensitivity of the simulations to subtleties of the numerics.
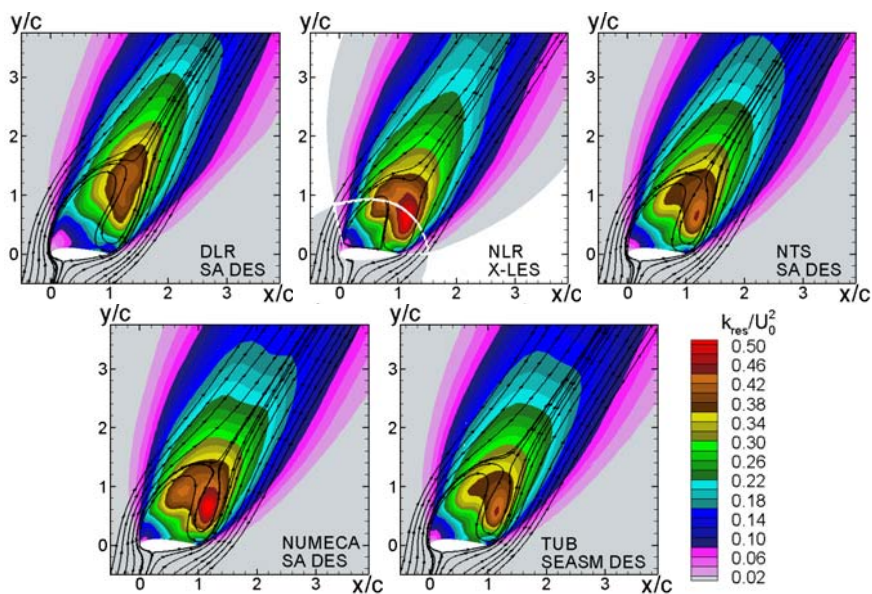

Figure 14 Comparison of mean flow streamlines and resolved turbulent kinetic energy computed by different partners (same simulations as in Fig.12)

3.5   SAS and TRRANS results and discussion

An essential common feature of these two, quite different, formulations is that both are of URANS-type, i.e., do not rely upon a size of computational cell as a model length-scale. Nonetheless, at least in massively separated flows, both approaches claim to possess a key LES feature, namely, a capability of resolving more and more fine turbulent structures with grid refinement. Simulations of the NACA0021 flow with the use of these approaches were performed by ANSYS (with the use of SAS) and NTS (with the use of SAS and TRRANS). Note that both partners used Version 2 of SAS based on the Menter-SST RANS model (see Section 1 of Chapter II for more detail). This version does involve a grid size and, as seen in Fig.15, where a snapshot is shown of the von-Karman length-scale from

the NTS coarse grid SAS, the equilibrium branch of this length-scale, $L_{vK, eq}$, the grid size enters in, turns out active in a significant part of the separation area and wake of the airfoil. This, strictly speaking, makes the model not a pure URANS one. However, the grid size is used only in the "max limiter", i.e., in a quite different manner than in DES and other hybrid RANS-LES models.
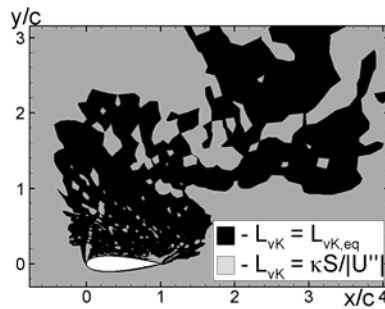

Figure 15 Snapshot of the von-Karman lengths-scale from SAS on NTS coarse grid

Figure 16 compares vorticity snapshots from SAS and TRRANS with those from SA DES at L_z=2c and 4c. The figure suggests that turbulence resolution provided by all the three modelling approaches is nearly the same. Also, no qualitative difference of the resolved vortical structures in *XY*-plane is observed between the simulations performed at L_z=2 and 4.
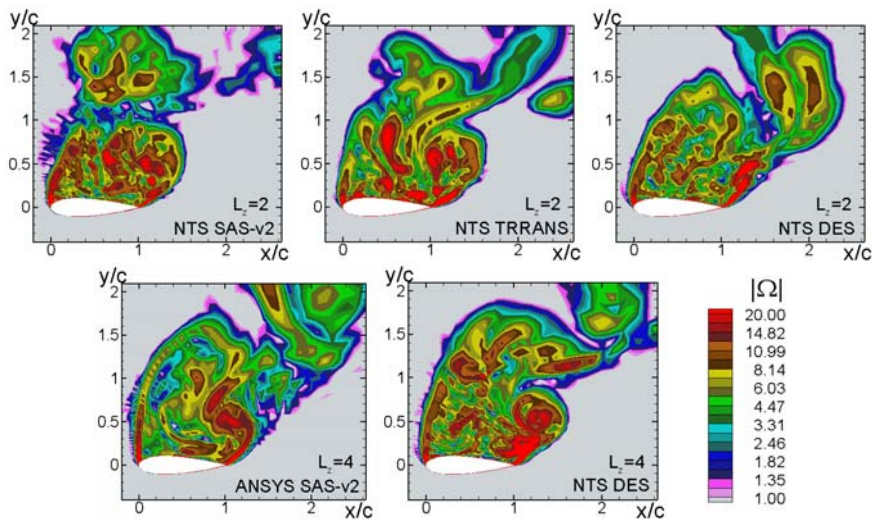

Figure 16 Comparison of vorticity snapshots from SAS, TRRANS, and SA DES. Simulations on the NTS coarse grid
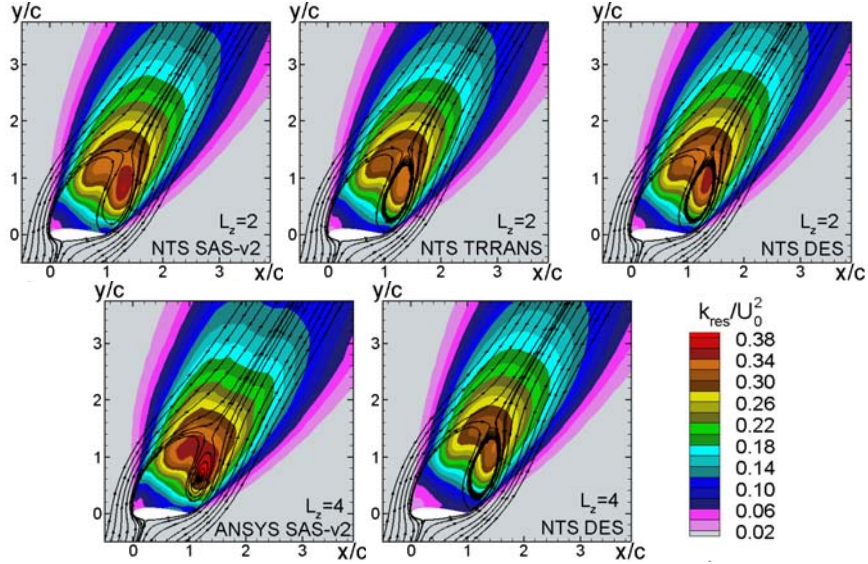
Figure 17 Comparison of mean streamlines and resolved kinetic energy from SAS,
TRRANS, and SA DES (same simulations as in Fig.16)

A similar conclusion can be drawn based on Fig.17, where the mean flow
topology (streamlines) and resolved turbulence kinetic energy fields are shown
from all the simulations. Still some difference between the modelling approaches
does exist, and SAS seems to result in somewhat higher resolved turbulence
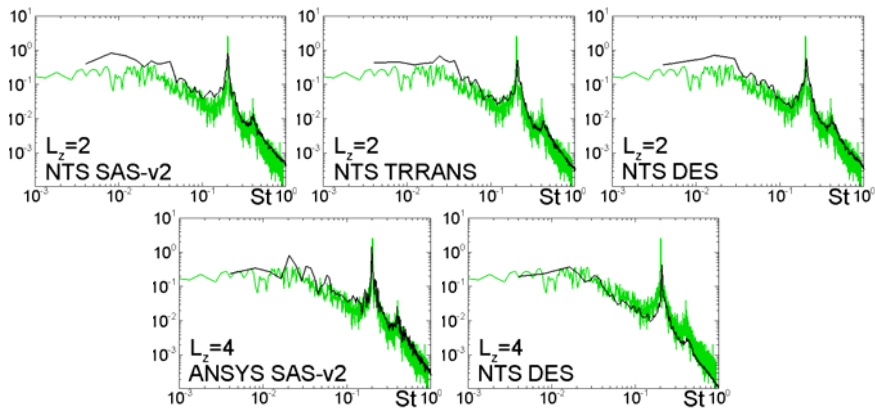kinetic energy than TRRANS and DES.

Figure 18 PSD of lift coefficient (same simulations as in Fig.16). Black lines –
simulations, green lines – data

Figure 18 compares PSD of the lift coefficient. One can see that, again, the different modelling approaches are in line with each other and predict both the broadband part of the spectra and the frequencies of the main and secondary peaks of C_L fairly well.
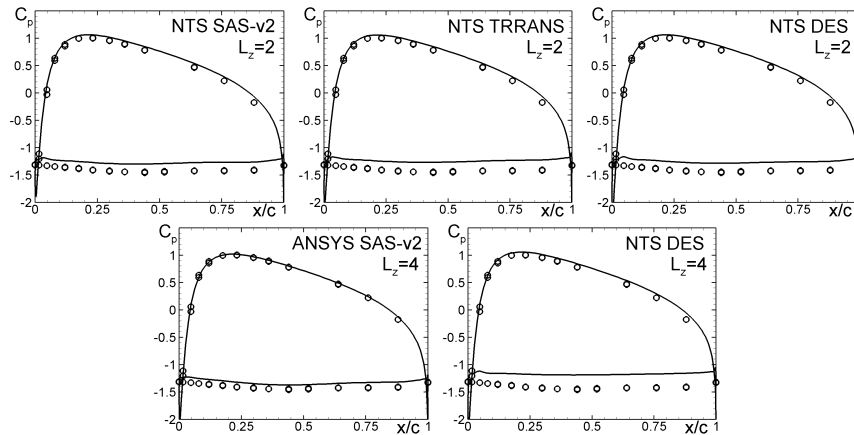

Figure 19 Mean pressure coefficient distributions (same simulations as in Fig.16)

Finally, Fig.19 compares distributions of the mean pressure coefficient over the airfoil from SAS, TRRANS, and DES. It shows that the distributions obtained by NTS at $L_z=2c$ are virtually identical, thus suggesting an equivalence of all the three approaches as applied to the considered flow. However, the figure also displays that at $L_z=2c$ the difference between SAS and DES is rather tangible. Moreover, as already mentioned, an increase of L_z from $2c$ up to $4c$ results in somewhat worse agreement of the DES predictions with the data, whereas the pressure distribution from ANSYS SAS at $L_z=4c$ agrees with the data fairly well. Unfortunately, neither SAS results of ANSYS at $L_z=2c$ nor those of NTS at $L_z=4c$ are available, which does not permit to tell whether the trend to an increase of the pressure on the suction side of the airfoil with L_z increase, typical of DES, holds valid for SAS or not.

3.6   Integral forces

Table 3 summarizes predictions of the integral lift and drag forces by the simulations performed by different partners. Note that only the results obtained with the longest available time samples, largest span sizes, and finest grids are included in the Table. Unfortunately, even some of these values (bold entries in the Table) are actually not sufficiently reliable in this sense (are obtained in the simulations with insufficient span-size or with too short time-samples). If not to take these values into consideration, the discrepancy of the lift and drag predictions with the data is within the range from ~2% (SST SAS at $L_z=4c$) up to ~10% (CEASM DES at $L_z=3.24$), which can be considered as reasonably good,

especially keeping in mind that the best RANS results for this kind of flow differ from the data by at least 25%.

Table 3 Summary of integral forces

Partner and approach	Lift, C_L	Drag, C_D
ANSYS (SST-SAS version 2, L_z=4, coarse NTS grid)	0.915	1.484
NTS (SST-SAS version 2, L_z=2, coarse NTS grid)	0.915	1.475
NTS (TRRANS, L_z=2, coarse NTS grid)	0.912	1.445
DLR (SA DDES with frozen filter, L_z=1, coarse NLR grid)	**1.001**	**1.548**
EADS-M (SA DES, fine EADS-M grid in wind-tunnel)	0.889	1.425
IMFT (k-ω OEM DES, L_z=1, coarse NTS grid)	**1.093**	**1.796**
NLR (X-LES, L_z=1, coarse NLR grid)	**1.108**	**1.613**
NTS (SA DES, L_z=4, coarse NTS grid)	0.879	1.381
NUMECA (SA DES, L_z=1, coarse NTS grid)	**1.026**	**1.688**
TUB (SALSA DES, L_z=1, coarse NTS grid)	**0.984**	**1.592**
TUB (LLR DES, L_z=1, coarse NTS grid)	**0.985**	**1.620**
TUB (CEASM DES, L_z=3.24, coarse NTS grid)	0.834	1.354
Experiment	*0.931*	*1.517*

3.7 Concluding remarks

As far as DES is concerned, in the course of DESider a representative database is accumulated on its performance as applied to this test case. Major findings from the simulations carried out by the partners are as follows.

A significant DES superiority over RANS in terms of the mean flow prediction and a marginal sensitivity of DES to a background RANS model are convincingly demonstrated, which supports similar observations based on the previous DES studies of airfoils in a deep stall. It is shown also that even relatively coarse grids of about 2M nodes are quite sufficient for getting virtually grid-independent mean flow characteristics. Also in line with the previous studies, it is shown that for getting a reliable statistics, very long time samples are needed (at least 300–400 convective time units, at least).

An important finding of the performed study is a strong sensitivity of DES predictions to the span-size of the computational domain and some worsening of the agreement of the predicted mean pressure and integral forces with the data when the span-size increases. This suggests that DES prediction of the mean characteristics of the flow is somewhat worse than it was believed earlier. In particular, the best (carried out with the very fine grid and accounting for the real geometry of the test section) simulation carried out by EADS-M underestimates the experimental integral lift and drag by 4.5% and 6% respectively. Although these errors are much less than those one would have with the use of the conventional (U)RANS modelling, this discrepancy with the data is still tangible. On the other hand, an opposite trend is observed with regard to the computed spectra of the lift and drag forces which agreement with the experimental spectra improves with the growth of the span-size of the domain. The reasons of this

contradictory behaviour of the mean and spectral flow characteristics are not clear and should be yet established.

For the SAS and TRRANS approaches, although the accumulated computational database is restricted by only two contributions (ANSYS and NTS), it still permits to make some important conclusions.

In particular, it is shown that as applied to the stalled airfoil flow, the approaches significantly surpass corresponding conventional RANS and URANS models and are quite competitive with DES. Also, based on the NTS experience, it can be concluded that the second version of the M-SST SAS is less numerics-sensitive and is compatible with "non-CFX" numerics.

Just as for DES, long time samples and large span-size of the domain are needed for an accurate prediction of the flow. In this respect, all the turbulence-resolving approaches are quite similar.

It should be noted also that the wide-domain (L_z=4c) SAS of ANSYS resulted in a better agreement with the data on the mean pressure distribution than both DES and TRRANS. Unfortunately, these results were obtained in the very end of the project, which did not permit to carry out additional simulations that could help to understand a reason of the observed difference.

References

Menter, F., Egorov, Y. (2005): A scale-adaptive simulation model using two-equation models, AIAA Paper, AIAA-2005-1095.

Shur, M., Spalart, P. R., Strelets, M., and Travin, A. (1999): Detached-Eddy Simulation of an Airfoil at High Angle of Attack. In: Proceedings of the 4th International Symposium on Engineering Turbulence Modeling and Measurements (W. Rodi and D. Laurence eds.) Elsevier, pp. 669–678.

Swalwell, K.E., Sheridan, J., and Melbourne W.H. (2003): Frequency Analysis of Surface Pressure on an Airfoil after Stall. Presented at the 21st AIAA Applied Aerodynamics Conference, AIAA Paper 2003-3416.

Swalwell, K.E. (2005): The Effect of Turbulence on Stall of Horizontal Axis Wind Turbines. Ph.D. Thesis. Monash University, October 2005.

Travin, A., Shur, M., Spalart, P.R., Strelets, M. (2004): On URANS solutions with LES like behaviour. In: Congress on Computational Methods in Applied Sciences and Engineering ECCOMAS 2004, P. Neittaanmäki, T.Rossi, K.Majava, and O.Pironneau (eds.). Jyväskylä, Finland, 24-28 July 2004.